Study of the signal response of the MÖNCH 25μm pitch hybrid pixel detector at different photon absorption depths

PUBLISHED BY IOP PUBLISHING FOR SISSA MEDIALAB
RECEIVED: *October 20, 2014*
REVISED: *December 16, 2014*
ACCEPTED: *January 7, 2015*
PUBLISHED: *March 16, 2015*

16th INTERNATIONAL WORKSHOP ON RADIATION IMAGING DETECTORS
22–26 JUNE 2014,
TRIESTE, ITALY

Study of the signal response of the MÖNCH 25μm pitch hybrid pixel detector at different photon absorption depths

S. Cartier,[a,b,1] **A. Bergamaschi,**[a] **R. Dinapoli,**[a] **D. Greiffenberg,**[a] **I. Johnson,**[a] **J.H. Jungmann-Smith,**[a] **D. Mezza,**[a] **A. Mozzanica,**[a] **X. Shi,**[a] **G. Tinti,**[a,c] **B. Schmitt**[a] **and M. Stampanoni**[a,b]

[a] *Swiss Light Source, Paul Scherrer Institute, Villigen, Switzerland*
[b] *Institute for Biomedical Engineering, University and ETH Zürich, Zürich, Switzerland*
[c] *ESRF, 6 Rue Horowitz, 38043 Grenoble, France*

E-mail: Sebastian.Cartier@psi.ch

ABSTRACT: MÖNCH is a 25 μm pitch hybrid silicon pixel detector with a charge integrating analog read-out front-end in each pixel. The small pixel size brings new challenges in bump-bonding, power consumption and chip design. The MÖNCH02 prototype ASIC, manufactured in UMC 110 nm technology with a field of view of 4×4 mm^2 and 160×160 pixels, has been characterized in the single photon regime, i.e. with less than one photon acquired per frame on average on a 3×3 pixel cluster. The low noise and small pixel size allow spatial interpolation with high resolution.

Understanding charge sharing as a function of the photon absorption depth and sensor bias is a key for optimal processing of single photon data for high resolution imaging. To characterize the charge collection of the detector, the sensor was illuminated with a 20 k*e*V photon beam in edge-on configuration at the SYRMEP beamline of Elettra. By slicing the beam by means of a 5 μm slit and scanning through the 320 μm silicon sensor depth, the charge collection is characterized as a function of the photon absorption depth for different sensor bias voltages.

KEYWORDS: Data processing methods; X-ray detectors; Detector modelling and simulations II (electric fields, charge transport, multiplication and induction, pulse formation, electron emission, etc)

[1] Corresponding author.

doi:10.1088/1748-0221/10/03/C03022

Contents

2015 JINST 10 C03022

1 Introduction

Several single photon counting (SPC) hybrid detectors like PILATUS [1], MYTHEN [2] and EIGER [3] are developed by the Paul Scherrer Institute (PSI, Villigen, Switzerland). They are in wide use at synchrotron facilities and provide a user-friendly, energy discriminating photon detection method for various applications [4]. Recently, mostly motivated by developing detectors for FEL applications, charge integrating (CI) detectors like GOTTHARD [5], JUNGFRAU [6] and MÖNCH [7] are investigated. Compared to SPC detectors the photon discrimination is no longer realized in each pixel of the read-out chip, but later by post-processing of the acquired images. This is achieved by integrating the charge produced by the detected photons during exposure in an analog circuit in each pixel. Later the integrated charge is sampled and then digitized off-chip by an analog-to-digital converter (ADC). CI detectors optimized for FEL applications typically have a dynamic range of 10^4 12 keV photons and are able to resolve single photons. PSI detectors achieve this high dynamic range by a technique called dynamic gain switching [5] and by low noise analog electronics to obtain a high signal-to-noise ratio (SNR).

Another interesting application for CI hybrid detectors is high resolution X-ray imaging at synchrotrons and X-ray tube sources. For these applications, position resolution requirements down to a few microns are usual. Therefore, indirect X-ray detection methods with the conversion of the X-rays in phosphor screens and charge collecting visible light imagers are currently still preferred [8]. The downside of indirect X-ray detection is low sensitivity. Therefore, a relatively high photon flux is needed to obtain enough signal-to-noise ratio in these indirect detection setups. Using direct detection methods can significantly reduce the needed flux because of the high signal response to single photons.

To fulfill the high resolution requirements and benefit from direct X-ray detection, we propose to operate a CI detector with low electronic noise and high gain in the single photon regime. Having a high gain reduces the dynamic range of the detector (in terms of the amount of detectable

photons per exposure), but allows to obtain energy-resolved information for each photon (which is particularly interesting in combination with polychromatic X-ray sources) and partial photon detection per pixel at low occupancies (short exposures and similar incoming photon rates). The partial detection of the charge of a photon in a pixel occurs because of the charge sharing effect. In the sensor, the charge cloud produced by an absorbed photon spreads out during the drift to the electrodes and will be detected by more than one pixel of the read-out chip. The position of impact of the photon can be obtained by analyzing the collected charge ratio in neighboring pixels.

R. Turchetta [9] started to investigate spatial resolution properties of silicon strip detectors to enhance particle tracking in high energy physics experiments. Other studies [10] investigated the charge sharing effect in silicon and gallium arsenide sensors with a Medipix1 chip [11] and photons up to 35 keV. At lower photon energies (up to $\sim$ 8 keV) charge-coupled devices (CCDs) under direct illumination of X-rays were investigated for high-resolution large area detectors with single photon resolution [12, 13] and for up to 17.4 keV sub-pixel resolution algorithms for fully depleted pn-junction CCDs with a pixel size of 75$\times$75 μm^2 were developed [14]. Centroiding algorithms also play an essential role for position reconstruction of signals from micro-channel plates (MCP) [15, 16]. We showed in previous studies [17–19] that it is possible to exploit the charge sharing effects to achieve sub-pixel position resolution in silicon hybrid strip and pixel detectors. Initially, we used CI and SPC strip detectors (GOTTHARD and MYTHEN) to investigate the charge sharing effect. Then, we extended the developed concepts for 2D-detectors.

In the presented work, we investigate the charge sharing effect in detail by looking at single photon events detected with the pixelated MÖNCH detector system at different photon absorption depths in the sensor. We address the charge sharing as a function of the absorption depth as the position resolution is dependent on this parameter. Furthermore, we investigate the influence of the electric field strengths on the resulting signal response of the detector by changing the applied sensor bias voltage. In section 2, we present the MÖNCH detector system in detail and we explain the proposed method to treat single photon events. In section 3, we outline the performed experiment, section 4 discusses the results and we draw conclusions from this study in section 5.

2 Materials and methods

2.1 MÖNCH detector

MÖNCH is a CI hybrid pixel detector developed at PSI. It is designated for applications as spectroscopy, resonant and non-resonant inelastic X-ray scattering and high resolution imaging experiments. MÖNCH has a small pixel pitch of 25$\times$25 μm^2 [7]. The sensor material (320 μm thick silicon in this study) is bump-bonded to the read-out chip. The analog CI and read-out circuit has a low noise of 30 e^- r.m.s. (prelimary results).

MÖNCH02 is a prototype ASIC (Application Specific Integrated Circuit) with a field of view (FOV) of 4$\times$4 mm^2 and a 160$\times$160 pixel matrix. Four different pixel groups are present on this prototype chip, each optimized for different applications. For this study, we focus on a 160$\times$40 pixel group (FOV of 1$\times$4 mm^2) which is targeting high resolution imaging. Continuous frame-rates up to 1 kHz are possible with the current prototype read-out board.

The prototype MÖNCH03 (submitted to the chip manufacturer) will have a field of view of 1$\times$1 cm^2 (160k pixels) and will be fully optimized for high resolution imaging. A new read-

2015 JINST 10 C03022

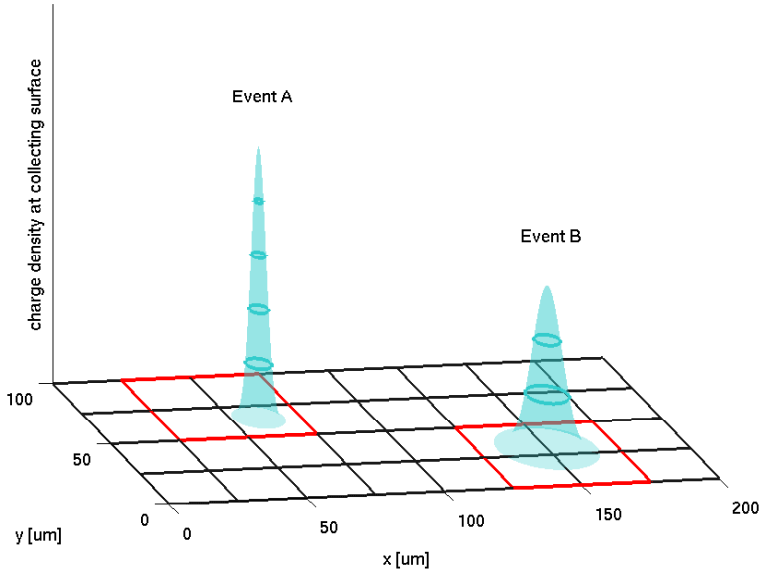

Figure 1. Visualization of the time integrated charge density at the collecting surface (blue) for two events at two different distances from the electrodes (event A is close, event B further away). Depending on the interaction depth, the charge density after diffusion is different, although the total amount of charge Q is the same for monochromatic photons. In the case of event A, the photon absorption was close to the electrodes and the charge had little time to drift. Therefore the charge density is high (concentrated at one spot) and most of the charge is collected by one pixel. For event B the charge cloud had more time to drift (absorption close to the backplane), the charge density is lower and the signal is detected by more than one pixel. 2×2 clusters found by the CFA are marked red.

out board is under development, which embeds two 10GbE connections and state-of-the-art field-programmable gate arrays (FPGAs). This will enable read-out speeds up to 8 kHz and the pre-compression of the data-stream to overcome network bandwidth limitations.

2.2 Cluster Finding Algorithm

Since our data frames have a low occupancy (by experimental design), for each detected photon we can first extract the region of interest by a cluster finding algorithm (CFA) [17] and then study the charge sharing behavior between neighboring pixels. In this study, we address the optimal size of the extracted clusters. To further understand the charge sharing effect, we calculate the collected charge ratio between the directly hit pixels and adjacent pixels in clusters. By knowing the distribution of this ratio as a function of the interaction depth, it is possible to draw conclusions about the average position information contained in such hits (figure 1). Many single frames with sparse hits (low occupancy) are required to get enough statistics to study the charge sharing behavior.

With incoming photon rates on the order of tens of photon per exposure, it is possible to extract isolated photon hits down to an energy of $\sim$ 1 keV (lower photon energies do not provide enough SNR). Due to charge sharing effects (induced mostly by charge diffusion in the sensor material), more than one pixel will detect the charge produced by the photon. To analyze this charge partitioning, we are interested in the signal values of pixels close to photon hits. The presented cluster

2015 JINST 10 C03022

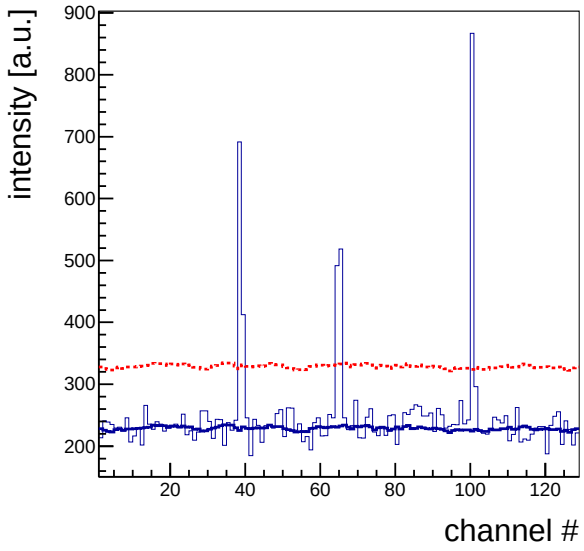

Figure 2. Simulated single frame snap-shot of a strip detector (1d-array). Blue: current signal level for each channel. Bold blue: moving average. Dashed red: moving threshold (moving average + 5 × standard deviation). A cluster is extracted if the signal level exceeds the running threshold. In this example frame, 3 photon hits are present.

finding algorithm extracts these areas from the acquired frames. A more detailed explanation of the CFA can be found in [17].

During exposure, CI detectors integrate not only signal produced by incident light but also sensor leakage current (also called dark current). To distinguish the signal generated by photons from this *dark image*, a pedestal is continuously updated for each pixel by a moving average over the last N empty frames (usually N $\sim$ 1000). This enables the compensation of drifts induced by temperature and other environmental changes. Since each pixel has its own CI circuitry, the resulting signals also differ in terms of noise properties. To account for that, the moving variance of the noise is calculated and used to compute the signal threshold. The threshold is fixed at 5 times the standard deviation of the obtained noise signal, giving a hit certainty over 99.9 % (figure 2 explains this in the one dimensional case). Once a pixel exceeds its threshold, a cluster of k×k pixels is extracted. In this study, we use clusters with 3 different sizes: 2×2, 3×3 and 5×5. To ensure that only one cluster is extracted per photon hit and hit overlaps are detected we enforce a minimal distance between extracted clusters.

2.3 In-cluster charge-ratio

To quantify the charge sharing effect within a cluster, we use the η-parameter defined as:

$$\begin{aligned} \eta^x_{i,j} &= (Q_{i+1,j} + Q_{i+1,j+1})/Q; \\ \eta^y_{i,j} &= (Q_{i,j+1} + Q_{i+1,j+1})/Q, \end{aligned} \tag{2.1}$$

for a single 2×2 cluster, where Q is the total charge collected in the cluster and $Q_{i+1,j} + Q_{i+1,j+1}$ and $Q_{i,j+1} + Q_{i+1,j+1}$, are the charges collected in the two north and east pixels of the 2×2 cluster, respectively [9].

2015 JINST 10 C03022

Analyzing the η-parameter of many photon absorption events at different positions in the sensor material by calculating the η-distribution $\left(\frac{dN}{d\eta}\right)$, enables to draw conclusions about the charge cloud drift in the sensor. Although the current read-out of the MÖNCH system introduces a slight difference in the η^x- and η^y-distribution (cross-talk caused by the limited speed of the read-out chain during the line-by-line based read-out) [17], we assume in this study that they are equal.

For hybrid detectors, the η-parameter is dependent on the absorption position in a non-linear way. To quantify the non-linearity of the η-parameter, we look at the peak-valley ratio (*PVR*) of the η-distribution:

$$PVR = \max\left(\frac{dN}{d\eta}\right) / \min\left(\frac{dN}{d\eta}\right). \tag{2.2}$$

In general a *PVR* close to 1 (indicating a flat η-distribution) shows that the investigated clusters contain more linear position information, and therefore the position reconstruction is simpler (see figure 6). In this study, we will look at absorption depth (z) dependent *PVR*s (denoted as $PVR(z)$).

3 Experimental setup

To control the interaction depth in the sensor, the detector system was edge-on illuminated by a monochromatic beam with 20 k*e*V photon energy at the Synchrotron Radiation for Medical Physics (SYRMEP) beamline, Elettra Sincrotrone, Trieste, Italy. The beam was additionally collimated by a 5 μm wide Tungsten slit (figure 3). With the X-ray source at 23 *m* distance [20] and a slit-to-detector distance of 10 *cm*, we can assume a nearly ideal box-illumination of 5 μm height. The relatively high photon energy of 20 k*e*V was chosen to penetrate the 500 μm wide guard ring (insensitive region of the sensor).

The sensor depth of 320 μm was scanned in 10 μm steps. At the backplane ($z = 0$) the charge cloud drifts through the entire sensor material, whereas closer to the electrode ($z = 300$ μm) the drift time is shorter. A 3-axis rotation stage enabled precise alignment of the detector surface to the beam. To investigate the charge drift at different electrical field strengths, we used two different sensor bias voltages of 90 V and 120 V.

At each step $500 \cdot 10^3$ frames with an exposure time of 12 μs were acquired. The short exposure time gives a high detector dead time of $\sim$ 99 %. The acquisition length for one scan step was 500 *s* at 1 k*Hz* frame rate.

4 Results

About $1.22 \cdot 10^6$ counts are detected per scan step with a step-to-step fluctuation of $\pm 89 \cdot 10^3$ for the scan at 90 V bias voltage ($1.12 \cdot 10^6 \pm 89 \cdot 10^3$ for 120 V).

In figure 4, the total collected charge of clusters (at scan position z) $Q(z)$ is compared to the total sum of 5×5 clusters at $z = 300$ μm (denoted Q_0) for two bias voltages. We assume that Q_0 contains all the charge produced by the photon hit. The collected charge at 120 V is always higher than at 90 V. Bigger clusters collect more charge than smaller. Currently, it is not clear what causes the the signal loss at small z for the 5×5 cluster. Read-out effects originating from a too

2015 JINST 10 C03022

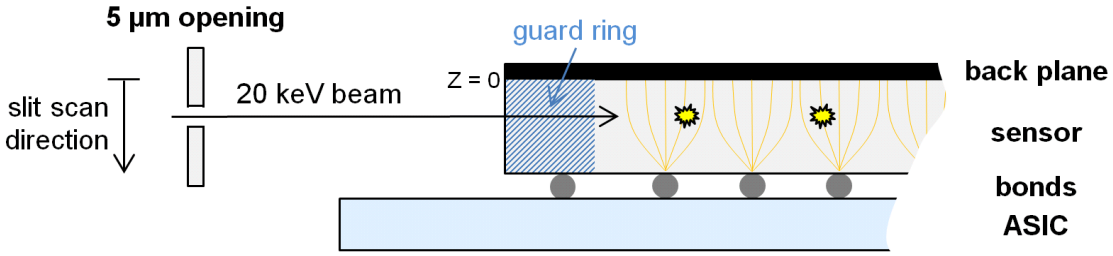

Figure 3. Setup of the sensor depth scan performed at SYRMEP: a collimated 20 keV beam (5 μm) is aligned horizontally to the sensor surface and scanned vertically trough the sensor volume. Schematic representation, not to scale.

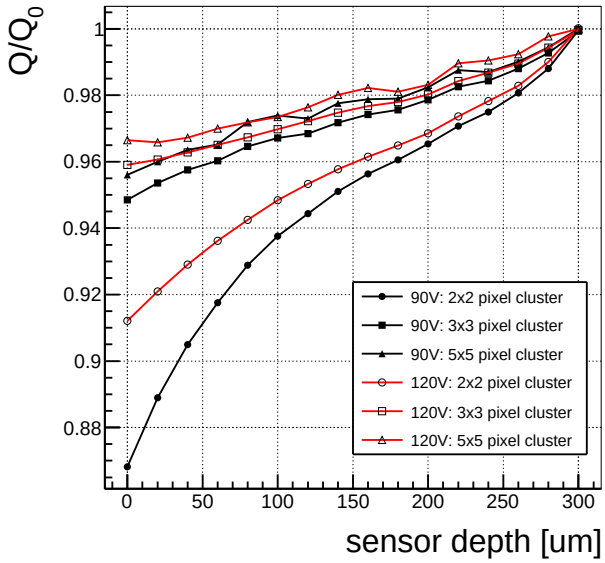

Figure 4. Comparison of the average collected charge in 2×2, 3×3 and 5×5 clusters at different interaction depths for two different sensor bias voltages.

slow read-out chain could cause a signal degradation if the charge is collected by many pixels and therefore lead to a signal loss at small z positions. Another contribution could be the relatively slow pre-amplifier in the pixels. It has a rise time of $\sim$ 1 μs, and therefore partial photon detection at the end of the exposure time is probable with an exposure time of 12 μs. The drift-time in the sensor (in the order of ten of nanoseconds) has most probably no significant impact on partial time-related photon detection. Close to the electrode the collected charge difference gets smaller between different cluster sizes and different bias voltages. The charge collection characteristics for 2×2 clusters has a non-linear dependency of the absorption depth z. At the backplane 13 % and 9 % of the charge is not collected by the small 2×2 cluster for 90 V and 120 V sensor bias, respectively. This may show that bigger clusters are beneficial for position reconstruction for lower X-ray energies or thicker sensors. Though, the noise introduced by the analog circuitry increases as well with bigger cluster sizes in these scenarios.

2015 JINST 10 C03022

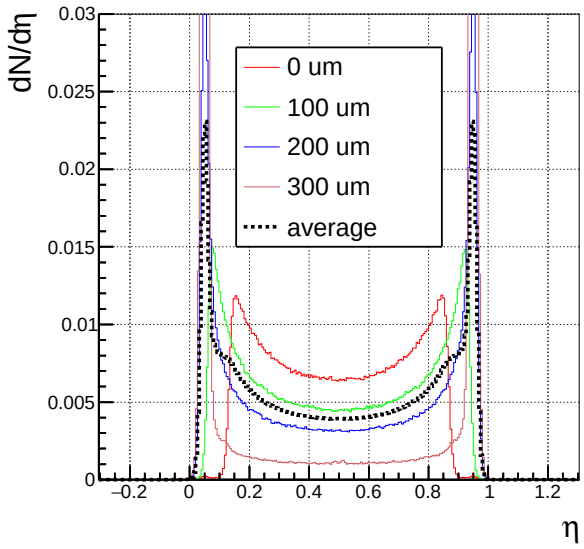

Figure 5. η-distribution at different interaction depths at 90 V bias voltage. The shape of the distribution changes, although the total amount of detected photons remains constant.

In figure 5, several η-distributions for different interaction depths are plotted. A small fraction of the events are outside the expected range of $\eta = (0,1)$. This occurs if the charge induced by a photon absorption is detected by only one pixel and all the adjacent pixels sample negative noise in this particular frame. It is also clearly visible that for higher z values, the peaks at the border are more prominent. Since the total amount of counts N is similar for all absorption depths, less counts are present in the center of the η-distribution. This effect is also clearly visible in the *PVR* comparison (figure 6). The shoulder of the peaks (most prominent for the averaged distribution in figure 5) is a geometric effect and can be investigated by using more complex charge collecting models (see [21]). For $z = 0$ hits with η close to 0 or 1 are rare, because the charge cloud diffuses more and is never detected by only one pixel.

The $PVR(z)$ for 120 V bias voltage is on average 30 % higher than for 90 V bias voltage (figure 6). This is mostly due to the faster charge collection time at higher electric field strengths. The *PVR* at $z = 300\ \mu$m for 90 V bias voltage is 47 times (35 times for 120 V) higher than at $z = 0$. If the photon interaction is further away from the electrode the *PVR* is lower and therefore the events contain more usable position information. We further conclude that thicker sensors would have more volume with low *PVR* and the position resolution is less dependent on the interaction depth. The average absorption depth is smaller for lower energies and the *PVR* is also lower.

5 Conclusions

The presented experiment and data analysis gives insight in the charge sharing effect in small pitch, pixelated silicon hybrid detectors like MÖNCH. We demonstrate that thicker sensor materials, are beneficial to further exploit charge sharing for high-resolution imaging, although thick sensors are more difficult to manufacture and operate (higher leakage current and higher depletion voltages). We also show that at lower sensor bias voltages, the charge sharing effect is more prominent and

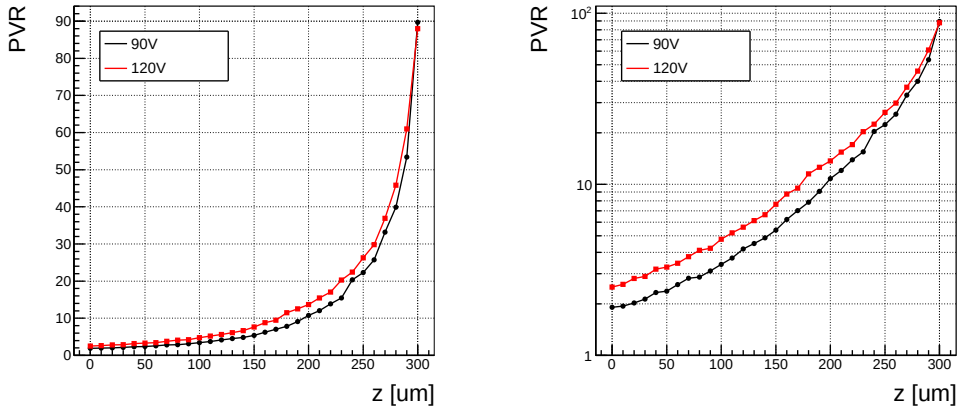

Figure 6. Change in η-distribution uniformity represented by the peak-value-ratio $PVR(z)$ at different interaction depths. Uniform η-distributions have a $PVR(z)$ equal to 1 (A linear, B logarithmic representation).

more position information can be extracted from each individual hit. We did not investigate the collecting behavior of partially depleted sensors.

Photons with lower energy are absorbed closer to the backplane in the sensor and the hits contain more position information, but the SNR is lower. If the photons are absorbed close to the read-out pad, only little position information can be extracted.

Although on average only 95 % of the charge is collected in a 2×2 cluster (at 90 V bias voltage), we conclude that this is the adequate cluster size for position reconstruction algorithms in the energy range around 20 keV. The results obtained in the presented experiment and others, motivate the development of a larger detector (MÖNCH03) with a FOV of 1×1 cm^2 (160k pixels) and higher frame rate for high resolution imaging.

Acknowledgments

The experiment presented in this study was conducted at the SYRMEP beamline of the Elettra Sincrotrone, Trieste, Italy (proposal #20135059). The authors acknowledge the support of the SYRMEP beamline staff in particular Fulvia Arfelli, Diego Dreossi, Renata Longo, Luigi Rigon and Nicola Sodini. The authors thank Dhanya Maliakal, Christian Ruder and Lukas Schädler for technical support.

References

[1] P. Kraft et al., *Performance of single-photon-counting PILATUS detector modules*, *J. Synchrotron Rad.* **16** (2009) 368.

[2] A. Bergamaschi et al., *The MYTHEN detector for X-ray powder diffraction experiments at the Swiss Light Source*, *J. Synchrotron Rad.* **17** (2010) 653.

[3] R. Dinapoli et al., *EIGER: next generation single photon counting detector for X-ray applications*, *Nucl. Instrum. Meth.* **A 650** (2011) 79.

2015 JINST 10 C03022

[4] A. Bergamaschi et al., *X-ray detector development at the Swiss Light Source*, *Synchrotron Radiat. News* **27** (2014) 3.

[5] A. Mozzanica et al., *The GOTTHARD charge integrating readout detector: design and characterization*, 2012 *JINST* **7** C01019.

[6] A. Mozzanica et al., *Prototype characterization of the JUNGFRAU pixel detector for SwissFEL*, 2014 *JINST* **9** C05010.

[7] R. Dinapoli et al., *MÖNCH, a small pitch, integrating hybrid pixel detector for X-ray applications*, 2015 *JINST* **9** C05015.

[8] M. Stampanoni et al., *Trends in synchrotron-based tomographic imaging: the SLS experience*, *SPIE Opt. Phot.* (2006) 63180M.

[9] R. Turchetta, *Spatial resolution of silicon microstrip detectors*, *Nucl. Instrum. Meth.* **A 335** (1993) 44.

[10] M. Sinor et al., *Charge sharing studies with a Medipix1 pixel device*, *Nucl. Instrum. Meth.* **A 509** (2003) 346.

[11] S.R. Amendolia et al., *MEDIPIX: a VLSI chip for a GaAs pixel detector for digital radiology*, *Nucl. Instrum. Meth.* **A 422** (1999) 201.

[12] F. Livet et al., *Using direct illumination CCDs as high-resolution area detectors for X-ray scattering*, *Nucl. Instrum. Meth.* **A 451** (2000) 596.

[13] K. Suhling et al., *Optimisation of centroiding algorithms for photon event counting imaging*, *Nucl. Instrum. Meth.* **437** (1999) 393.

[14] A. Abboud et al., *Sub-pixel resolution of a pnCCD for X-ray white beam applications*, 2013 *JINST* **8** P05005.

[15] A. Kharchenko et al., *Sparse spectral techniques for emission imaging*, *Int. J. Mass Spectrom.* **351** (2013) 37.

[16] A.S. Tremsin et al., *Spatial distribution of electron cloud footprints from microchannel plates: measurements and modeling*, *Rev. Sci. Instrum.* **70** (1999) 3282.

[17] S. Cartier et al., *Micron resolution of MÖNCH and GOTTHARD, small pitch charge integrating detectors with single photon sensitivity*, 2014 *JINST* **9** C05027.

[18] A. Schubert et al., *Micrometre resolution of a charge integrating microstrip detector with single photon sensitivity*, *J. Synchrotron. Rad.* **19** (2012) 359.

[19] A. Bergamaschi et al., *Performance of a single photon counting microstrip detector for strip pitches down to 10μm*, *Nucl. Instrum. Meth.* **A 591** (2008) 163.

[20] A. Abrami et al., *Medical applications of synchrotron radiation at the SYRMEP beamline of ELETTRA*, *Nucl. Instrum. Meth.* **A 548** (2005) 221.

[21] A. Bergamaschi et al., *Looking at single photons using hybrid detectors*, 2015 *JINST* **10** C01033.

2015 JINST 10 C03022